

UNC5C variants are associated with cerebral amyloid angiopathy

OPEN

Hyun-Sik Yang, MD
Charles C. White, PhD
Lori B. Chibnik, PhD
Hans-Ulrich Klein, PhD
Julie A. Schneider, MD
David A. Bennett, MD
Philip L. De Jager, MD,
PhD

Correspondence to
Dr. De Jager:
pld2115@cumc.columbia.edu

ABSTRACT

Objective: To determine whether common genetic variants in *UNC5C*, a recently identified late-onset Alzheimer disease (LOAD) dementia susceptibility gene, are associated with AD susceptibility or AD-related clinical/pathologic phenotypes.

Methods: We used data from deceased individuals of European descent who participated in the Religious Orders Study or the Rush Memory and Aging Project ($n = 1,288$). We examined whether there were associations between single nucleotide polymorphisms (SNPs) within ± 100 kb of the *UNC5C* gene and a diagnosis of AD dementia, global cognitive decline, a pathologic diagnosis of AD, β -amyloid load, neuritic plaque count, diffuse plaque count, paired helical filament tau density, neurofibrillary tangle count, and cerebral amyloid angiopathy (CAA) score. We also evaluated the relation of the CAA-associated variant and dorsolateral prefrontal cortex (DLPFC) *UNC5C* RNA expression. Secondary analyses were performed to examine the interaction of the CAA-associated SNP and known genetic risk factors of CAA as well as the association of the SNP with other cerebrovascular pathologies.

Results: A set of *UNC5C* SNPs tagged by rs28660566^T was associated with a higher CAA score ($p = 2.3 \times 10^{-6}$): each additional rs28660566^T allele was associated with a 0.60 point higher CAA score, which is equivalent to approximately 75% of the higher CAA score associated with each allele of *APOE* $\epsilon 4$. rs28660566^T was weakly associated with lower *UNC5C* expression in the human DLPFC ($p = 0.036$). Moreover, rs28660566^T had a synergistic interaction with *APOE* $\epsilon 4$ on their association with higher CAA severity ($p = 0.027$) and was associated with more severe arteriolosclerosis ($p = 0.0065$).

Conclusions: Targeted analysis of the *UNC5C* region uncovered a set of SNPs associated with CAA. *Neuro Genet* 2017;3:e176; doi: 10.1212/NXG.000000000000176

GLOSSARY

AD = Alzheimer disease; **CAA** = cerebral amyloid angiopathy; **CI** = confidence interval; **DLPFC** = dorsolateral prefrontal cortex; **LD** = linkage disequilibrium; **LOAD** = late-onset Alzheimer disease; **MAF** = minor allele frequency; **MAP** = Rush Memory and Aging Project; **OR** = odds ratio; **PHFtau** = paired helical filament tau; **QC** = quality control; **RNA-Seq** = RNA-sequencing; **ROS** = Religious Orders Study; **SNP** = single nucleotide polymorphism.

A recent study reported the association of *UNC5C* T835M (rs137875858^A), a rare coding variant in this netrin receptor implicated in axon guidance during development,¹ with late-onset Alzheimer disease (LOAD).² As we have shown in our study of the *TREM* locus,³ multiple genetic variants in the same locus can have independent effects on disease susceptibility and could affect specific features of the disease. We, therefore, assessed whether common *UNC5C* variants influence AD-related cognitive and pathologic phenotypes in 2 large clinical pathologic cohort studies of aging and dementia. We found a set of *UNC5C* single nucleotide

Supplemental data
at Neurology.org/ng

From the Departments of Neurology and Psychiatry (H.-S.Y., C.C.W., H.-U.K., P.L.D.J.), Program in Translational NeuroPsychiatric Genomics, Institute for the Neurosciences; Department of Neurology (H.-S.Y.), Center for Alzheimer Research and Treatment, Brigham and Women's Hospital; Harvard Medical School (H.-S.Y., H.-U.K.); Harvard T.H. Chan School of Public Health (L.B.C.), Boston; Program in Medical and Population Genetics (H.-S.Y., C.C.W., L.B.C., H.-U.K., P.L.D.J.), Broad Institute, Cambridge, MA; Rush Alzheimer's Disease Center (J.A.S., D.A.B.) and Department of Neurological Sciences (J.A.S., D.A.B.), Rush University Medical Center, Chicago, IL; and Department of Neurology (P.L.D.J.), Center for Translational & Systems Neuroimmunology, Columbia University Medical Center, New York, NY.

Funding information and disclosures are provided at the end of the article. Go to Neurology.org/ng for full disclosure forms. The Article Processing Charge was funded by the authors.

This is an open access article distributed under the terms of the Creative Commons Attribution-NonCommercial-NoDerivatives License 4.0 (CC BY-NC-ND), which permits downloading and sharing the work provided it is properly cited. The work cannot be changed in any way or used commercially without permission from the journal.

polymorphisms (SNPs) in a single linkage disequilibrium (LD) block linked to the severity of cerebral amyloid angiopathy (CAA), a disease of small cerebral arterioles caused by β -amyloid accumulation.⁴

METHODS **Subjects, standard protocol approvals, registrations, and patient consents.** Our subjects were from 2 large community-based cohort studies of older adults, the Religious Orders Study (ROS) and the Rush Memory and Aging Project (MAP).^{5,6} Both studies enroll older adults without known dementia, and each participant signed written informed consent and Anatomical Gift Act. All study steps were done in compliance with the protocol approved by the Rush University Medical Center Institutional Review Board. Overall follow-up rate and autopsy rate for deceased individuals were greater than 85%. Of note, these 2 cohorts were designed to be used in combined analyses: ROS and MAP were designed and managed by the same team of investigators at the Rush Alzheimer's Disease Center and captured shared phenotypic measures. We limited our analyses to deceased European-descent individuals with quality-controlled genome-wide genotyping data and completed autopsy (February 2016 Data Freeze, total $n = 1,288$).

Cognitive and pathologic phenotypes. Nine AD-related cognitive and pathologic variables (diagnosis of AD dementia, global cognitive decline, pathologic diagnosis of AD, β -amyloid load, neuritic plaque count, diffuse plaque count, paired helical filament tau [PHFtau] density, neurofibrillary tangle count, and the CAA score) were defined as previously described.^{3,5-7} Square-root transformed values were used for analyses of continuous pathologic variables (β -amyloid load, neuritic plaque count, diffuse plaque count, PHFtau density, and neurofibrillary tangle count) to account for their positively skew deviation, as previously described.³ CAA was graded on a 5-point scale (0–4) in 4 neocortical regions (dorsolateral prefrontal cortex [DLPFC], angular gyrus, inferior temporal gyrus, and calcarine cortex) and averaged to derive a CAA score (0–4).⁷ Of note, among the 1,288 subjects in this study, numbers of subjects with measured values for each phenotype, who were included in each analysis, were as follows: diagnosis of AD dementia ($n = 1,257$), global cognitive decline ($n = 1,193$), pathologic diagnosis of AD ($n = 1,140$), β -amyloid load ($n = 1,095$), neuritic plaque count ($n = 1,132$), diffuse plaque count ($n = 1,132$), PHFtau density ($n = 1,088$), neurofibrillary tangle count, ($n = 1,132$), and CAA score ($n = 1,107$).

For secondary analyses, atherosclerosis, arteriosclerosis, gross infarcts, and microinfarcts are measured as previously described.⁸ In brief, atherosclerosis was assessed by visual inspection at the circle of Willis, and the severity was semiquantitatively graded (scale from 0 to 6), which was collapsed into 4 levels (none/possible, mild, moderate, and severe) for analysis. Arteriosclerosis was microscopically evaluated in anterior basal ganglia with a semiquantitative scale (0–7), which was collapsed into 4 levels (none, mild, moderate, and severe) for analysis. Gross infarcts and microinfarcts were recorded as present vs absent. Among the 1,288 subjects in this study, numbers of subjects with measured values for each phenotype, who were included in each analysis, were as follows: atherosclerosis ($n = 1,141$), arteriosclerosis ($n = 1,130$), gross infarcts ($n = 1,136$), and microinfarcts ($n = 1,136$).

Genotyping and RNA-Seq data acquisition and processing. Genome-wide genotyping (on either Affymetrix GeneChip 6.0 or Illumina OmniQuad Express), quality control (QC), and imputation

were performed as previously described.³ Genotype QC was done with PLINK software version 1.08,⁹ and the metrics included a genotype success rate of $>95\%$, Hardy-Weinberg $p > 0.001$, and a misshap test of $<1 \times 10^{-9}$. Closely related individuals are removed with Pihat method using PLINK. EIGENSTRAT (default setting)¹⁰ was used to generate a genotype covariance matrix, and population outliers were removed. Then, genotype imputation was done with BEAGLE software (version 3.3.2)¹¹ on a reference map from 1,000 Genomes Project Consortium interim phase I haplotypes (2010–2011 data freeze). Imputed genotypes with a minor allele frequency (MAF) of >0.01 and an INFO score of >0.3 were used in this analysis. We defined the *UNC5C* region as the chromosomal segment containing the transcribed elements of *UNC5C* and ± 100 kb of flanking DNA (chr4: 95,983,655-96,570,361 on hg19 build), which contained 2,269 1000 Genomes Project reference SNPs. Of note, *APOE* genotypes were measured through a separate sequencing procedure as previously described,^{5,6} and *APOE* $\epsilon 2$ and $\epsilon 4$ allele counts were used in this study. RNA was extracted from frozen postmortem DLPFC from a subset of participants and was quantified using next-generation quantitative RNA-sequencing (RNA-Seq). QC and quantile normalization of RNA-Seq Fragments Per Kilobase of transcript per Million fragments mapped (FPKM) values for *UNC5C* were done as previously described,¹² and 494 subjects in our study had nonmissing values.

Statistical analyses. Statistical analyses were performed with R 3.2.1 (r-project.org), and we combined ROS and MAP in all our analyses, unless otherwise specified. To derive the number of independent genetic markers tested in this study, we used LD-based SNP pruning (with an r^2 threshold of 0.2, a window of 50 SNPs, and a step of 5 SNPs), done with PLINK, as previously published.³ This procedure yielded 391 independent LD blocks within the *UNC5C* region. As we tested for 9 traits, Bonferroni-adjusted α for the primary analysis was $\alpha = 1.4 \times 10^{-5}$ ($0.05 \div [391 \times 9]$). Assuming additive genetic effects, logistic regression models were used for dichotomous outcome variables (AD dementia and pathologic AD), and linear regression models were used for others, with covariates including age at death, sex, cohort (ROS vs MAP), and the first 3 principal components from the genotype covariance matrix derived with EIGENSTRAT. Years of education was also included as a covariate in the analyses of phenotypes affected by cognitive performance (AD dementia and global cognitive decline). Results from 2 genotyping platforms were calculated separately and meta-analyzed with PLINK, and the consistencies across genotyping platforms were examined with meta-analyses I^2 values.¹³ The results were plotted using LocusZoom,¹⁴ with chromatin state tracks predicted by the ChromHMM core 15-chromatin state model¹⁵ from the Roadmap Epigenomics Project.¹⁶

For SNPs associated with a trait (CAA), we looked up the LD r^2 values between the lead SNP and all other identified SNPs in the HaploReg database¹⁷ and also analyzed each of the other SNPs in a same linear model with the lead SNP to examine whether they represent a different LD block or not. The population variance explained by the lead SNP was derived from a sequential adjusted R-squared analysis with linear models: We first calculated the adjusted R-squared from a linear model to explain the trait of interest with age at death, sex, study cohort, genotyping platform, and first 3 principal components from the genotype covariance matrix. Then, we included the lead SNP's minor allele dosage in the model and calculated the increment of the adjusted R-squared. The population variance explained by the SNP was then compared with that of *APOE* $\epsilon 4$.

To further evaluate the functional significance of the LD block associated with increased CAA severity, we examined the

predicted chromatin state (per the ChromHMM core 15-chromatin state model from the Roadmap Epigenomics Project^{15,16}) of each SNP associated with CAA severity. Then, the lead SNP was tested for the association with the *UNC5C* RNA level in a linear model, controlling for age at death, sex, study cohort, genotyping platform, first 3 principal components from the genotype covariance matrix, and technical covariates (RNA integrity score, log₂(total aligned reads), postmortem interval, and number of ribosomal bases). Then, the *UNC5C* RNA level was tested for its association with CAA severity, controlling for the same set of covariates.

In addition, to test whether the association between the identified *UNC5C* variant and CAA is independent of known genetic risk factors for CAA (*APOE* ε4, ε2, and *CRI* rs6656401^A),¹⁸ each of the previously reported genetic risk factors was added to the linear model testing association between the *UNC5C* variant and the CAA score. Interaction between the *UNC5C* variant and a previously reported genetic risk factor was checked using the product term in the linear regression model, if the association of the *UNC5C* variant and the CAA score attenuated after including that known genetic risk factor in the model. After the statistical interaction was found, stratified analysis was done to further test the relationship between 2 genetic risk factors. Of note, we assumed an additive effect of CAA severity by *APOE* ε4, ε2, or *CRI* rs6656401^A in our models.

Further exploratory analyses were performed to interrogate the association of the identified *UNC5C* CAA variant and cerebrovascular pathology. Ordinal logistic regression models were used for the ordered categorical variables (atherosclerosis and arteriolosclerosis), and logistic regression models were used for the binary variables (gross infarct and microinfarct). Age at death, sex, study cohort, genotyping platform, and first 3 principal components from the genotype covariance matrix were included as covariates for each analysis. *p* values were Bonferroni adjusted for multiple comparisons (number of testing = 4 for these targeted exploratory analyses).

Finally, the sample size required to reproduce our result was calculated with the Genetic Power Calculator, assuming an additive model and a similar effect size.¹⁹

RESULTS Demographic characteristics of the subjects are summarized in table 1. The total number of subjects analyzed in this study was *n* = 1,288. Among the subjects, 1,114 were genotyped with

Affymetrix GeneChip 6.0, and 174 were genotyped with Illumina OmniQuad Express. In our primary analyses using additive models, 10 *UNC5C* intronic SNPs were associated with a higher CAA score (*p* < 1.4 × 10⁻⁵) (figure 1 and table 2). All 10 SNPs were imputed SNPs with good imputation quality (INFO score > 0.89; table e-1 at Neurology.org/ng), and the association was consistent across genotyping platforms, shown by meta-analysis *I*² = 0 for all 10 SNPs. No other associations are found between *UNC5C* variants and other tested AD-related traits (*p* > 5.0 × 10⁻⁴ for all other trait-SNP pairs, well above the threshold type I error rate of this study; figure e-1).

The top CAA risk allele rs28660566^T (MAF = 3.6%) was in LD with the other 9 identified SNPs (*r*² ≥ 0.36, *D'* ≥ 0.93; table 2). To rule out their effect independent of rs28660566^T, each of the 9 SNP dosages was tested in a same linear additive model with rs28660566^T, and none were associated with the CAA score when adjusted for rs28660566^T (*p* > 0.05). Thus, rs28660566^T tags all other SNPs associated with a higher CAA score, and this LD block defines a chromosomal segment containing several *UNC5C* exons (figure 1). In the linear model, the presence of an rs28660566^T allele corresponded to a 0.60-point higher CAA score, which is approximately 75% of the effect size of an *APOE* ε4 allele on this trait (estimated effect 0.80, *p* = 1.5 × 10⁻³⁸). The *UNC5C* variant therefore has a large effect, but rs28660566^T (MAF 3.6%) explained approximately only 1.9% of the population variance given its low MAF, whereas *APOE* ε4 (MAF 13.8%) explained approximately 13.1% of the population variance. Of note, rs28660566^T dosage was not associated with parenchymal β-amyloid load (*p* = 0.80).

The predicted chromatin state of a given chromosomal segment (table 2 and figure 1) can be helpful in inferring its functional implications (e.g., enhancer, promoter, etc.). The lead SNP rs28660566^T was within a chromosomal region identified as an enhancer in multiple brain regions, suggesting that this region may have a regulatory role. None of the other identified SNPs were in the regulatory chromosomal region in the DLPFC. Of interest, rs28660566^T dosage was nominally associated with decreased *UNC5C* mRNA expression in the DLPFC (estimated effect -0.097, 95% confidence interval [CI] -0.19 to -0.0063, *p* = 0.036), but the DLPFC *UNC5C* mRNA expression level was not associated with the CAA score (*p* = 0.75).

APOE ε4, ε2, and *CRI* rs6656401^A have been previously reported to be associated with higher odds and/or severity of CAA.¹⁸ The association between rs28660566^T and the CAA score was attenuated by

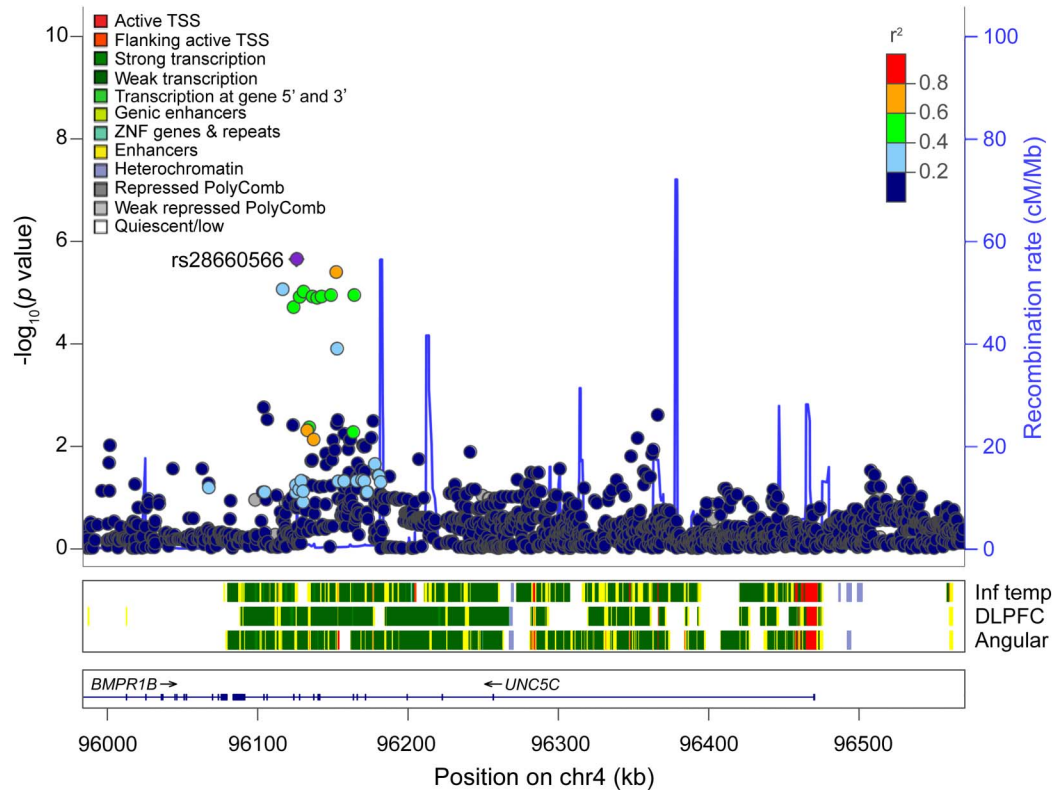
Table 1 Demographic characteristics of the subjects

	ROS	MAP	Combined	Nonmissing
Cohort size, n	614	674	1,288	NA
Age at death, mean (SD)	87.8 (6.9)	89.8 (6.0)	88.9 (6.5)	1,288
Sex, female, n (%)	383 (62.4)	456 (67.7)	839 (65.1)	1,288
Education, y (SD)	18.2 (3.4)	14.4 (2.8)	16.3 (3.64)	1,287
Diagnosis of AD dementia, n (%)	261 (43.4)	246 (37.5)	507 (40.3)	1,257
Pathologic diagnosis of AD, n (%)	361 (62.7)	360 (63.8)	721 (63.2)	1,140
CAA, median (IQR)	0.75 (1.5)	0.75 (1.5)	0.75 (1.5)	1,107

Abbreviations: AD = Alzheimer disease; CAA = cerebral amyloid angiopathy; IQR = interquartile range; MAP = Rush Memory and Aging Project; NA = not applicable; ROS = Religious Orders Study.

Nonmissing indicates number of participants with measured values in the combined cohort, who are included in the genetic association study for each trait.

Figure 1 Regional association plot of the CAA score in the *UNC5C* region



Regional association plots of CAA in *UNC5C* ± 100 kb. X-axis denotes chromosomal location on chromosome 4, and Y-axis denotes negative log of the p value of the association between the SNP and the CAA score, adjusting for age at death, sex, study cohort, and first 3 principal components from the genetic covariance matrix. Each point corresponds to each SNP, and the color of each point indicates linkage disequilibrium r^2 value between each SNP of interest and rs28660566^T. Blue line in the graph represents recombination rate in cM/Mb. The color-coded tracks below the association plot show predicted functional chromatin states in inferior temporal cortex (Inf Temp), DLPFC, and angular gyrus cortex (angular), derived from the Roadmap Epigenomics project. CAA = cerebral amyloid angiopathy; DLPFC = dorsolateral prefrontal cortex; TSS = transcription start site; ZNF = zinc finger. The track below the predicted chromatin states shows the location of genes: the thick line is exon, and the thin line is intron.

approximately 13% when the *APOE* $\epsilon 4$ allele count was included in the model (estimated effect 0.52, 95% CI 0.29–0.75, $p = 1.2 \times 10^{-5}$). In fact, a statistical interaction between *APOE* $\epsilon 4$ allele count and rs28660566^T dosage on the CAA score was present, suggesting a synergistic effect modification between these 2 genetic risk factors (estimated effect 0.44, 95% CI 0.049–0.84, $p = 0.027$). In a stratified analysis, the association between rs28660566^T dosage and the CAA score was weaker in a subgroup with no *APOE* $\epsilon 4$ allele ($n = 822$, estimated effect 0.38, 95% CI 0.12–0.64, $p = 0.0046$) compared with the association in a subgroup with 1 or 2 *APOE* $\epsilon 4$ alleles ($n = 285$, estimated effect 1.00, 95% CI 0.50–1.50, $p = 1.2 \times 10^{-4}$). By contrast, the association between rs28660566^T and the CAA score did not change by adding *APOE* $\epsilon 2$ or *CRI* rs6656401^A in the model (with *APOE* $\epsilon 2$: estimated effect 0.60; 95% CI 0.35–0.85; $p = 2.0 \times 10^{-6}$, with rs6656401^A: estimated effect 0.60; 95% CI 0.35–0.85; $p = 2.3 \times 10^{-6}$).

In an additional exploratory analysis to test whether rs28660566^T alters the relationship between parenchymal β -amyloid load and the CAA score, we found no statistically significant interaction between rs28660566^T and parenchymal β -amyloid load on their associations with the CAA score ($p = 0.42$). Then, we also explored whether rs28660566^T was associated with other cerebrovascular pathologies (Bonferroni-corrected p value threshold 0.0125): rs28660566^T was associated with increased odds of more severe arteriolosclerosis (odds ratio [OR] 1.8; 95% CI 1.2–2.8; $p = 0.0065$) but not with atherosclerosis (OR 1.6; 95% CI 1.1–2.4; $p = 0.023$), gross infarcts ($p = 0.54$), or microinfarcts ($p = 0.69$).

Finally, we calculated the sample size required to replicate our result with the Genetic Power Calculator,¹⁹ assuming a similar effect size. Assuming an additive model with 4% of MAF, 389 subjects are needed to detect 2% of total population variance with a type I error rate of 0.05 and power of 80%.

Table 2 SNPs associated with the severity of CAA

SNP	Chr4 POS	MAF	LD (r ²)	Estimated effect (95% CI)	p Value	Chromatin state		
						Inf temp	DLPFC	Angular
rs28660566 ^T	96,125,762	0.036	NA	0.60 (0.35-0.85)	2.3 × 10 ⁻⁶	Enh	Enh	Enh
rs11941383 ^T	96,151,958	0.042	0.76	0.52 (0.30-0.74)	4.1 × 10 ⁻⁶	TxWk	TXWk	TxWk
rs140160653 ^A	96,116,350	0.017	0.36	0.78 (0.44-1.13)	8.8 × 10 ⁻⁶	Enh	TxWk	EnhG
rs77321857 ^T	96,130,211	0.022	0.52	0.69 (0.38-1.00)	9.8 × 10 ⁻⁶	Quies	TxWk	TxWk
rs74590670 ^G	96,163,984	0.022	0.52	0.69 (0.38-1.00)	1.1 × 10 ⁻⁵	Tx	Tx	TxWk
rs139069750 ^G	96,148,504	0.022	0.52	0.69 (0.38-1.00)	1.2 × 10 ⁻⁵	TxWk	TxWk	TxWk
rs138877862 ^C	96,136,118	0.022	0.46	0.69 (0.38-0.99)	1.2 × 10 ⁻⁶	TxWk	TxWk	TxWk
rs75985930 ^A	96,142,169	0.022	0.46	0.69 (0.38-0.99)	1.2 × 10 ⁻⁶	Enh	TxWk	TxWk
rs75083968 ^A	96,127,609	0.022	0.52	0.69 (0.38-0.99)	1.2 × 10 ⁻⁵	Quies	TxWk	TxWk
rs147682457 ^A	96,139,245	0.022	0.52	0.68 (0.38-0.99)	1.3 × 10 ⁻⁵	TxWk	TxWk	TxWk

Abbreviations: Angular = angular gyrus; CAA = cerebral amyloid angiopathy; CI = confidence interval; DLPFC = dorso-lateral prefrontal cortex; Enh = enhancers; EnhG = genic enhancers; Inf Temp = inferior temporal cortex; LD = linkage disequilibrium; MAF = minor allele frequency; MAP = Rush Memory and Aging Project; Quies = Quiescent/low; ROS = the Religious Orders Study; SNP = single nucleotide polymorphism; Tx = strong transcription; TxWk = weak transcription. In the combined ROS-MAP cohort, linear regression model was used to assess the association of each genotype with the CAA score, adjusting for age at death, sex, study cohort, and first 3 principal components from the population covariance matrix. Estimated effect indicates estimated CAA score increase per each minor allele of the SNP of interest. Chr4 POS shows chromosomal position of each SNP per hg19 reference map. Chromatin state shows predicted chromatin state in 3 cortical regions available from the Roadmap Epigenomics data set and ChromHMM algorithm (core 1.5-state model), in the chromosomal region where the SNP is located. LD(D') = 1 and meta-analyses I² = 0 across genotyping platforms for all SNPs in this table.

DISCUSSION Targeted analysis of the chromosomal region of *UNC5C*, a recently identified AD susceptibility gene, uncovered a possible new risk locus associated with CAA severity, which comprises a single LD block captured by rs28660566^T. Of interest, rs28660566^T synergistically interacts with *APOE* ε4 to increase CAA severity, suggesting a possibility of a common downstream pathway.

In a recent study reporting the association of a rare *UNC5C* coding variant rs137875858^A (*UNC5C* T835M) with LOAD, the authors showed that *UNC5C* T835M exerts its effect through increased neuronal vulnerability rather than increased amyloid or tau production.² Consistent with this report, no common *UNC5C* variant was associated with parenchymal β-amyloid or PHFtau accumulation in our study. Thus, the association of *UNC5C* rs28660566^T with CAA is more likely to be mediated by ineffective perivascular β-amyloid drainage rather than increased neuronal β-amyloid production. Of interest, rs28660566^T was also associated with arteriosclerosis, a disease of small deep cerebral arterioles, suggesting an implication of *UNC5C* in arteriolar susceptibility to pathologic changes, not only limited to vascular β-amyloid deposition. In fact, a previous study reported that *UNC5C* is expressed in endothelial cells, and inhibition of *UNC5C* attenuated netrin-1 effect on in vitro endothelial cell migration,²⁰ suggesting a potential role of *UNC5C* in vascular development and maintenance.

The functional mechanism of the *UNC5C* CAA severity risk locus remains to be determined. The lead SNP, rs28660566^T, is located within a predicted enhancer chromosomal locus in multiple brain regions,^{15,16} and in our study, it was a weak eQTL associated with lower *UNC5C* mRNA expression in the DLPFC. However, the DLPFC *UNC5C* mRNA level was not associated with CAA severity. Nonetheless, our DLPFC RNA-Seq data lack cell-type specific information and might not capture differential expression limited to certain tissue types such as arterioles. As CAA is a disease primarily of small cortical and leptomeningeal arterioles,⁴ gene expression profiles from isolated leptomeningeal and cortical arterioles might be necessary to further dissect the mechanisms of *UNC5C* in CAA progression.

Of note, the previously reported *UNC5C* T835M variant (chromosome 4, position 96,091,431) is 34.3 kb away from rs28660566^T, and it is not included in the chromosomal segment defined by the LD block captured by rs28660566^T. *UNC5C* T835M might be on a same haplotype with rs28660566^T, given the low recombination frequency between the 2 loci (figure 1), but we cannot confirm this in ROS-MAP participants because the sequencing of the *UNC5C* region is not yet available. However, given the rarity of T835M (MAF <0.1%), it is very unlikely that the observed association is driven by *UNC5C* T835M in our subject population (n = 1,107 for the CAA analysis). We also note that rs28660566^T is not in LD with rs3846455^G

(237.3 kb apart from rs28660566¹), an *UNC5C* allele that we have recently reported to be associated with worse late-life cognition, when adjusted for the burden of multiple neuropathologies (including CAA) and demographics.²¹ Thus, there are both allelic and phenotypic heterogeneity within the *UNC5C* locus, similar to our previous findings in the *TREM* locus.³

The study is methodologically robust. The analyses are performed on more than 1,100 participants from 2 community-based cohort studies, with a semiquantitative assessment of CAA severity in multiple cortical regions. We performed a targeted gene analysis of *UNC5C*, and a set of *UNC5C* variants showed significant association with the CAA severity after rigorously correcting for the number of hypotheses tested. Moreover, the result was consistent across 2 genotyping platforms. Validation efforts with independent data sets are essential to extend the evaluation of this risk locus, and close to 400 subjects with pathologic assessment of CAA in multiple cortical areas are required to replicate our findings with type 1 error rate of 0.05 and power of 80%. In addition, experimental studies would be essential to understand the underlying biological mechanisms. In conclusion, we found an *UNC5C* variant to be associated with CAA severity, and additional studies are required to clarify the role of *UNC5C* in CAA pathogenesis.

AUTHOR CONTRIBUTIONS

Hyun-Sik Yang and Charles C. White: drafting/revising the manuscript for content, study concept or design, statistical analysis, and analysis or interpretation of data. Lori B. Chibnik: drafting/revising the manuscript for content, study concept or design, and analysis or interpretation of data. Hans-Ulrich Klein: drafting/revising the manuscript for content and analysis or interpretation of data. Julie A. Schneider and David A. Bennett: drafting/revising the manuscript for content, analysis or interpretation of data, acquisition of data, and obtaining funding. Philip L. De Jager: drafting/revising the manuscript for content, study concept or design, analysis or interpretation of data, acquisition of data, study supervision, and obtaining funding.

ACKNOWLEDGMENT

The authors thank the study participants. More information regarding obtaining (ROS/MAP/ROS and MAP) data for research use can be found at the RADC Research Resource Sharing Hub (radc.rush.edu).

STUDY FUNDING

The study was funded by NIH grants P30AG10161, R01AG17917, R01AG036836, R01AG15819, and U01AG046152.

DISCLOSURE

H.-S. Yang has received research support from Alzheimer's Association Clinical Fellowship. C.C. White reports no disclosures. L.B. Chibnik has received research support from NIH/NIA. H.-U. Klein reports no disclosures. J.A. Schneider has served on scientific advisory boards for Alzheimer's Association, Fondation Plan Alzheimer (France), the Dutch CAA Foundation, University of Washington/Group Health Alzheimer's Disease Patient Registry/Adult Changes in Thought study, New York University, AVID Radiopharmaceuticals, Genentech, Grifols, and Eli Lilly; has served on the editorial boards of the *Journal of Histochemistry & Cytochemistry* and the

Journal of Neuropathology & Experimental Neurology; has been a consultant for AVID Radiopharmaceuticals, Navidea Biopharmaceuticals Inc., the Michael J. Fox Foundation, National Football League, and National Hockey League; has received research support from AVID Radiopharmaceuticals, NIH, and NIA; and has taken part in legal proceedings involving National Football League, National Hockey League, and World Wrestling Entertainment. D.A. Bennett has served on scientific advisory boards for Vigorous Minds, Takeda Pharmaceuticals, and AbbVie; has served on the editorial boards of *Neurology*, *Current Alzheimer Research*, and *Neuroepidemiology*; and has received research support from NIH. P.L. De Jager has served on scientific advisory boards for TEVA Neuroscience, Genzyme/Sanofi, and Celgene; has received speaker honoraria from Biogen Idec, Source Health care Analytics, Pfizer Inc., and TEVA; has served on the editorial boards of the *Journal of Neuroimmunology*, *Neuroepigenetics*, and *Multiple Sclerosis*; and has received research support from Biogen, Eisai, UCB, Pfizer, Sanofi/Genzyme, NIH, NIA, and the National MS Society. Go to Neurology.org/ng for full disclosure forms.

Received March 21, 2017. Accepted in final form June 6, 2017.

REFERENCES

1. Leonardo ED, Hinck L, Masu M, Keino-Masu K, Ackerman SL, Tessier-Lavigne M. Vertebrate homologues of *C. elegans* UNC-5 are candidate netrin receptors. *Nature* 1997;386:833–838.
2. Wetzel-smith MK, Hunkapiller J, Bhangale TR, et al. A rare mutation in *UNC5C* predisposes to late-onset Alzheimer's disease and increases neuronal cell death. *Nat Med* 2014;20:1452–1457.
3. Replogle JM, Chan G, White CC, et al. A *TREM1* variant alters the accumulation of Alzheimer-related amyloid pathology. *Ann Neurol* 2015;77:469–477.
4. Charidimou A, Gang Q, Werring DJ. Sporadic cerebral amyloid angiopathy revisited: recent insights into pathophysiology and clinical spectrum. *J Neurol Neurosurg Psychiatry* 2012;83:124–137.
5. Bennett DA, Schneider JA, Arvanitakis Z, Wilson RS. Overview and findings from the Religious Orders Study. *Curr Alzheimer Res* 2012;9:628–645.
6. Bennett DA, Schneider JA, Buchman AS, Barnes LL, Boyle PA, Wilson RS. Overview and findings from the rush Memory and aging project. *Curr Alzheimer Res* 2012;9:646–663.
7. Boyle PA, Yu L, Nag S, et al. Cerebral amyloid angiopathy and cognitive outcomes in community-based older persons. *Neurology* 2015;85:1930–1936.
8. Arvanitakis Z, Capuano AW, Leurgans SE, Buchman AS, Bennett DA, Schneider JA. The relationship of cerebral vessel pathology to brain microinfarcts. *Brain Pathol* 2017; 27:77–85.
9. Purcell S, Neale B, Todd-Brown K, et al. PLINK: a tool set for whole-genome association and population-based linkage analyses. *Am J Hum Genet* 2007;81:559–575.
10. Price AL, Patterson NJ, Plenge RM, Weinblatt ME, Shadick NA, Reich D. Principal components analysis corrects for stratification in genome-wide association studies. *Nat Genet* 2006;38:904–909.
11. Browning BL, Browning SR. A unified approach to genotype imputation and haplotype-phase inference for large data sets of trios and unrelated individuals. *Am J Hum Genet* 2009;84:210–223.
12. Chan G, White CC, Winn PA, et al. CD33 modulates *TREM2*: convergence of Alzheimer loci. *Nat Neurosci* 2015;18:1556–1558.

13. Higgins JP, Thompson SG, Deeks JJ, Altman DG. Measuring inconsistency in meta-analyses. *BMJ* 2003;327:557–560.
14. Pruim RJ, Welch RP, Sanna S, et al. LocusZoom: regional visualization of genome-wide association scan results. *Bioinformatics* 2010;26:2336–2337.
15. Ernst J, Kellis M. ChromHMM: automating chromatin-state discovery and characterization. *Nat Methods* 2012;9:215–216.
16. Roadmap Epigenomics C, Kundaje A, Meuleman W, et al. Integrative analysis of 111 reference human epigenomes. *Nature* 2015;518:317–330.
17. Ward LD, Kellis M. HaploReg: a resource for exploring chromatin states, conservation, and regulatory motif alterations within sets of genetically linked variants. *Nucleic Acids Res* 2012;40:D930–D934.
18. Biffi A, Shulman JM, Jagiella JM, et al. Genetic variation at CR1 increases risk of cerebral amyloid angiopathy. *Neurology* 2012;78:334–341.
19. Purcell S, Cherny SS, Sham PC. Genetic Power Calculator: design of linkage and association genetic mapping studies of complex traits. *Bioinformatics* 2003;19:149–150.
20. Lejmi E, Leconte L, Pedron-Mazoyer S, et al. Netrin-4 inhibits angiogenesis via binding to neogenin and recruitment of Unc5B. *Proc Natl Acad Sci USA* 2008;105:12491–12496.
21. White CC, Yang HS, Yu L, et al. Identification of genes associated with dissociation of cognitive performance and neuropathological burden: Multistep analysis of genetic, epigenetic, and transcriptional data. *PLoS Med* 2017;14:e1002287.